frontiers | Frontiers in Chemical Engineering

TYPE Original Research
PUBLISHED 20 August 2025
DOI 10.3389/fceng.2025.1580201

OPEN ACCESS

EDITED BY
Chirangano Mangwandi,
Queen's University Belfast, United Kingdom

REVIEWED BY
Jayato Nayak,
Mahindra University, India
Jarosław Serafin,
University of Barcelona, Spain

*CORRESPONDENCE
Gamunu Samarakoon,
gamunu.arachchige@usn.no

RECEIVED 20 February 2025
ACCEPTED 01 July 2025
PUBLISHED 20 August 2025

CITATION
Jayasinghe T, Amarasooriya G, Kawakami T, Sivalingam V and Samarakoon G (2025) Hexavalent chromium (Cr^{6+}) removal from wastewater through electrolysis: Influence of Al^{3+}, Fe^{3+}, and Mg^{2+} ion additives on treatment efficiency.
Front. Chem. Eng. 7:1580201.
doi: 10.3389/fceng.2025.1580201

Hexavalent chromium (Cr^{6+}) removal from wastewater through electrolysis: Influence of Al^{3+}, Fe^{3+}, and Mg^{2+} ion additives on treatment efficiency

Thilini Jayasinghe[1], Gayan Amarasooriya[1], Tomonori Kawakami[2], Vasan Sivalingam[3] and Gamunu Samarakoon[4]*

[1]Faculty of Applied Sciences, Uva Wellassa University of Sri Lanka, Badulla, Sri Lanka, [2]Faculty of Engineering, Toyama Prefectural University, Toyama, Japan, [3]Sweco Norge AS, Seljord, Norway, [4]Faculty of Technology, Natural Sciences and Maritime Sciences, University of South-Eastern Norway, Porsgrun, Norway

Introduction: A type of batch electrolysis system comprising a platinum anode and stainless-steel cathode was investigated for the removal of hexavalent chromium (Cr^{6+}) from synthetic wastewater.

Methods: Electrochemical treatment was conducted at a constant current of 0.25 A with NaCl of 1 g/L as the supporting electrolyte.

Results: The highest Cr^{6+} removal efficiencies achieved were at 100 mg/L metal ion dosage and an initial Cr^{6+} concentration of 5 mg/L, yielding removal rates of 56.80% for Fe^{3+}, 49.62% for Al^{3+}, and 30.05% for Mg^{2+}.

Discussion: Removal was attributed to the in-situ formation of metal hydroxides ($Al(OH)_3$, $Fe(OH)_3$, $Mg(OH)_2$), which subsequently enhanced the reduction and immobilization of Cr^{6+} through co-precipitation, Coulomb forces, and electrostatic adsorption. Further increase in Cr^{6+} removal efficiency was inhibited at higher initial Cr^{6+} concentrations due to the saturation of hydroxides, which also exhibited competitive behaviour toward ion adsorption. These results confirm the significant role of multivalent cation additives in increasing the remediation of Cr^{6+} in the electrochemical system, thus lending support to the theory behind the development of scalable additive-assisted electrochemical water treatment technique.

KEYWORDS

electrolysis, Al^{3+}, Fe^{3+}, Mg^{2+}: co-precipitation, coulomb forces

1 Introduction

The term 'wastewater' refers to the liquid waste products generated by a community, encompassing typical human waste from residences and workplaces, as well as various waste products and compounds from commercial and industrial activities. Among these contaminants, heavy metals such as lead, nickel, copper, and chromium possess numerous toxic properties that harm humans and the environment.

When considering chromium, it is a metal that can be hazardous and cancer-causing, resulting from both anthropogenic and natural processes. The two primary forms of

chromium released into aquatic systems are Trivalent Chromium (Cr^{3+}) and Hexavalent Chromium (Cr^{6+}). Chromium compounds, made using sodium/potassium dichromate as a base material, are released in enormous quantities into the environment (Carneiro et al., 2019). Chromium compounds have gained extensive applications in wood preservation, printing inks, textile dyeing, leather tanning, paints, pigments, and metal plating (Krishnani et al., 2013).

Chromium can be ingested through the skin, consumed, and inhaled by humans. Animal and human tissues are known to collect Cr^{3+} and Cr^{6+}. Developmental problems, including growth retardation and neurodevelopmental impairments, as well as harm to the skin, respiratory, reproductive, and digestive systems, and an increased risk of cancer, are some of the hazardous effects of chromium compounds on humans and animals (Aitio et al., 1984). Cr^{6+} has been shown in studies to be hazardous even at low concentrations (Chen et al., 2024; Kerur et al., 2020; Park et al., 2022). These include deadly toxicity, behavioural modifications, and decreased growth, reproduction, and survival in invertebrates (Zhou et al., 2021; Hamadeen et al., 2022). They also include reduced growth and photosynthesis in algae and aquatic plants. Hexavalent chromium exposure in fish has resulted in altered physical and metabolic conditions, longer hatching times, DNA damage, and lower survival rates (Kumar Saha and Ghosh, 2022; Kokkinos et al., 2019; Merical, 2007). Consequently, chromium must be removed from wastewater for environmental conservation and reuse in the material recycling in the existing circular economy systems. Almost all countries, including the World Health Organization (WHO), have set recommended safe discharge limits for chromium (Yan et al., 2023).

Usually, Cr^{6+} is extremely mobile and soluble throughout a wide pH range, increasing its potential for migration and harmfulness (Chen et al., 2024). Compared to Cr^{6+}, Cr^{3+} has roughly 500–1,000 times less toxicity and mobility, and is very simple to remove by precipitation and adsorption (Park et al., 2022; Golder et al., 2007; Costa, 2003). Therefore, one essential technique for treating wastewater containing chrome is reducing Cr^{6+} to Cr^{3+} (Yogeshwaran and Priya, 2018). Although the traditional adsorption method is easy to use, it can be hard to use on a wide scale because adsorbents' pores (such as activated carbon, zeolite, resin, etc.) are prone to clogging and have low regeneration effectiveness (Mohan and Pittman, 2006). Other methods include solvent extraction, membrane separators, reverse osmosis, ion exchange, biodegradation, adsorption by natural biomaterials like fungi and algae, biosorption, coagulation, and electrochemical treatments such as electrocoagulation, electroreduction, and electrodeionization (Peng et al., 2019; Malinovic et al., 2022; Zongo et al., 2009; Garg et al., 2023).

Electrocoagulation (EC) has been recognized for its efficiency, cost-effectiveness, and environmental compatibility in treating wastewater. It involves the electrolytic dissolution of electrodes (usually aluminum or iron) to generate coagulants that aid in flocculation and contaminant removal. The process utilizes electrons as the primary reagents, making it productive and economically viable (Malinovic et al., 2022; Characterization et al., 2020).

On the other hand, Electrolysis (ELC) has been noted for its ability to generate chlorine gas (Cl_2) and hydrogen gas (H_2) through an electrolytic process that maintains high pH and low pH solutions in separate compartments via a permeable diaphragm (Amarasooriya and Kawakami, 2020). This technique offers advantages, including reduced electrode dissociation and enhanced process efficiency, through the application of Coulombic forces.

While EC commonly employs sacrificial metal electrodes (e.g., aluminum or iron), releasing coagulants (Malinovic et al., 2022), ELC often utilizes inert electrodes to facilitate redox reactions and coagulant generation, either indirectly or through external addition. Both have proven effective for Cr^{6+} removal; however, most studies focus on sacrificial electrodes where electrodes serve as reagents.

The use of non-sacrificial electrodes such as platinum anodes and stainless-steel cathodes in combination with externally added coagulants (e.g., Al^{3+}, Fe^{3+}, Mg^{2+}) remains largely unexplored. Although these inert materials do not contribute coagulants directly, they may offer significant advantages in terms of electrode durability, process control, and sustainability. Despite their potential, the impact of such configurations on the performance of EC and ELC systems for Cr^{6+} removal has not been systematically studied.

This study addresses this critical gap by investigating the removal efficiency of Cr^{6+} from wastewater using an electrolysis system configured with platinum and stainless-steel electrodes, supplemented with different coagulant agents. The system was assessed under various operational conditions to evaluate the influence of coagulant type and electrochemical configuration.

The novelty of this work lies in employing non-sacrificial electrode materials with externally optimized coagulant dosing, providing new insights into electrochemical process performance, cost-effectiveness, and long-term operational sustainability. These findings contribute to expanding the toolkit for advanced wastewater treatment technologies aligned with circular economy and resource recovery strategies.

2 Materials and methods

2.1 Chemicals and instruments

In this work, different concentrations of synthetic aqueous solutions of Cr^{6+} and, as a coagulant agent, Fe^{3+}, $Al^{3+,}$ and Mg^{2+} were used in the ELC reactor. A 1000 mg/L synthetic stock solution of Cr^{6+} was prepared by dissolving 2.829 g of $K_2Cr_2O_4$ (HCN Code 28415000- India) in 1 L of distilled water. 5 mg/L, 10 mg/L and 20 mg/L of Cr^{6+} solutions were prepared by proper dilutions. 1,000 mg/L stock solution of Al^{3+} was prepared by dissolving 8.970 g of $AlCl_3.6H_2O$ (HCN Code 2827320000- India) in 1 L of distilled water. 1000 mg/L stock solution of Fe^{3+} was prepared by dissolving 2.904 g of $FeCl_3$ (HCN Code 282739- India) in 1L of distilled water. 1,000 mg/L stock solution of Mg^{2+} was prepared by dissolving 8.470 g of $MgCl_2.6H_2O$ (HSN Code 28273100- India) in 1 L of distilled water. Working concentrations of Fe^{3+}, Al^{3+}, and Mg^{2+} (5 mg/L to 100 mg/L) were prepared by Cr^{6+} synthetic stock solution. NaCl 1 g/L was added as an electrolyte to enhance the solution's conductivity. The pH of the samples was measured by using a laboratory pH meter (HANNA, USA, HI 2020-02). The analytical measurements of chromium, aluminum, iron, and

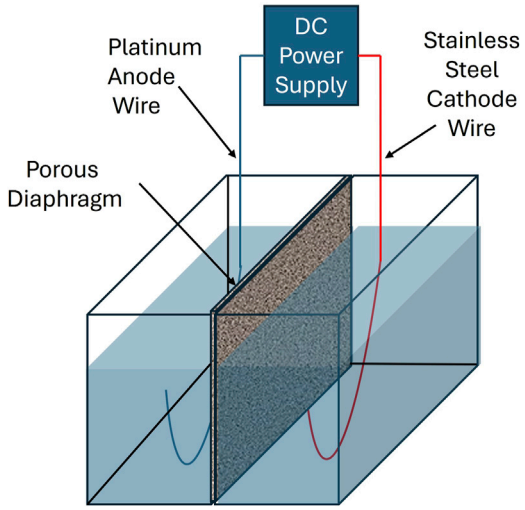

FIGURE 1
Experimental setup.

magnesium was performed by the Atomic Absorption Spectrophotometer (Varian AA 240 FS atomic absorption spectrometer- USA). The concentration of chromium in aqueous samples was determined using AAS at a wavelength of 357.9 nm, which corresponds to the most sensitive line for chromium detection. A series of calibration standards was prepared from a 1,000 mg/L certified Chromium stock solution by serial dilution to obtain concentrations of 0.5, 1, 2, 5, 10, and 20 mg/L. The calibration curve exhibited excellent linearity with a correlation coefficient (R^2) greater than 0.999, confirming the accuracy of quantification across the working range. To ensure the precision and reliability of measurements, calibration was repeated after every 10 samples to monitor for potential instrumental drift.

2.2 Experimental Setup

All electrolysis experiments were performed in a square-shaped cell having two equal compartments of a plastic cell (H:7.5 × W: 10.5 × L:15.0 cm^3). The compartments were named as anode and cathode. The anode and cathode volumes were equally separated by using a permeable clay diaphragm and this diaphragm allows both cations and anions transferred through the anode and cathode without any special ion selectivity (Figure 1). The diaphragm prevents the mixing of sludge produced in the cathode and helps in the separation of anode and cathode solutions. A platinum wire electrode was used as an anode, and a single stainless-steel electrode was used as a cathode at an inter-electrode distance of 5 cm for all experiments with a constant current power source. The Pt electrode was purchased from the Nilaco Corporation, Japan, and the stainless-steel electrode was obtained from the local market in Sri Lanka. Platinum (anode) and stainless steel (cathode) were selected as inert, non-sacrificial electrodes to prevent contamination from electrode dissolution, enhance process stability, and allow precise control over coagulant dosing. This configuration supports long-term sustainability and minimizes maintenance compared to traditional sacrificial electrodes. A constant current of 0.25 A was applied for 30 min during each electrolysis run with 600 mL of synthetic solution. These conditions were selected based on preliminary experimental trials that demonstrated effective Cr^{6+} removal and stable performance across all test scenarios. Although full optimization was not performed, these parameters provided a consistent and practical baseline for evaluating the effects of different coagulants. After each run, 50 mL of water was collected from each anode and cathode cell to measure the ion concentrations. All experiments were independently performed in triplicate (n = 3) for each condition to ensure reproducibility, and the results are presented as the average of these replicates.

3 Results and discussion

3.1 Baseline Cr^{6+} removal by electrolysis without coagulant additives

To establish a performance baseline, control experiments were conducted without the addition of Al^{3+}, Fe^{3+}, or Mg^{2+} ions. The Cr^{6+} removal efficiency of the electrolysis system alone was evaluated at initial Cr^{6+} concentrations of 5, 10, and 20 mg/L under constant charge loading (25 mA for 30 min = 1500 C/L). Removal was primarily driven by cathodic reduction, with cathodic efficiencies of 17.77%, 9.88%, and 14.65%, respectively. Anodic removal was minimal or negative, and appreciable precipitative removal (14.24%) occurred only at the highest Cr^{6+} concentration (20 mg/L), likely due to localized hydroxide formation enabling $Cr(OH)_3$ precipitation. These results confirm that while electrolysis alone can reduce Cr^{6+} levels to some extent, the presence of coagulant ions is essential to enhance removal efficiency and support stable precipitation mechanisms.

3.2 Effect of the initial Al^{3+} concentration on the removal of Cr^{6+}

The removal efficiency of Cr^{6+} in the synthesized wastewater was investigated by keeping the charge loading (C/L) constant (25 mA for 30 min = 1500 C/L) for initial chromium concentrations of 5 mg/L, 10 mg/L, and 20 mg/L. Further, for different Cr^{6+} levels, the initial coagulant Al^{3+} concentration was varied from 0 mg/L to 100 mg/L. The influence of the initial Al^{3+} concentration on the removal efficiency of Cr^{6+} at initial Cr^{6+} concentrations of 5 mg/L, 10 mg/L, and 20 mg/L is depicted in Figures 2a–c, respectively. The respective pH variations in the anode and cathode baths are shown in Figures 3a–c. Equation 1 was employed for calculating Cr^{6+} removed by precipitation from the total system (Anode + Cathode).

$$\text{Chromium removal percentage by precipitation} = [(Ci\text{-}Cc) - (Ca\text{-}Ci)] / Ci \times 100\% \quad (1)$$

Where,

Ci: Initial Cr^{6+} Concentration in the cathode and anode (mg/L).

Ca: Final Cr^{6+} Concentration in the anode (mg/L).

Cc: Final Cr^{6+} Concentration in the cathode (mg/L).

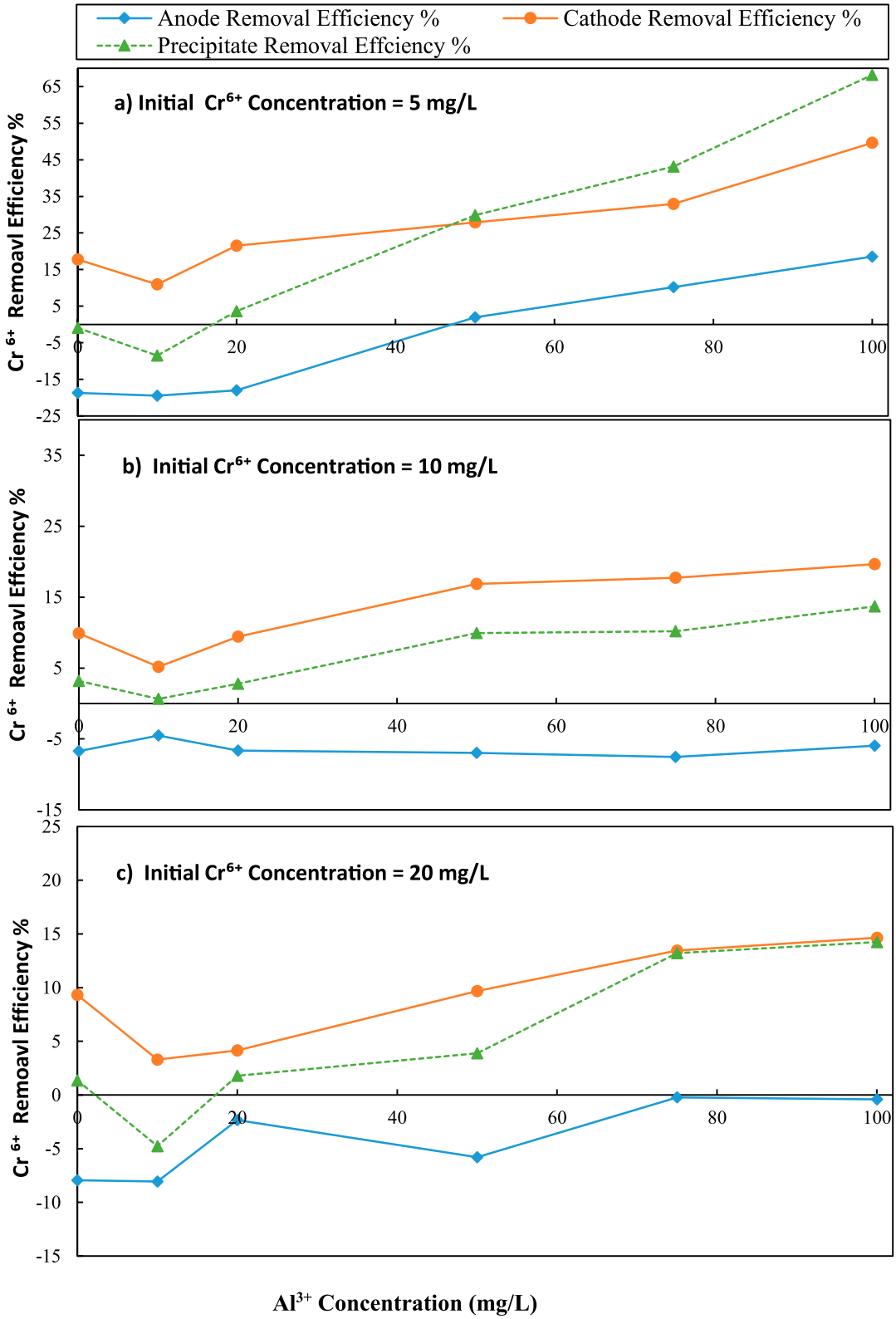

FIGURE 2
Variation of Cr^{6+} removal with initial Al^{3+} concentration over different initial Cr^{6+} concentration **(a)** 5 mg/L, **(b)** 10 mg/L and **(c)** 20 mg/L; C/L applied at = 1500 C/L (0.25 A)

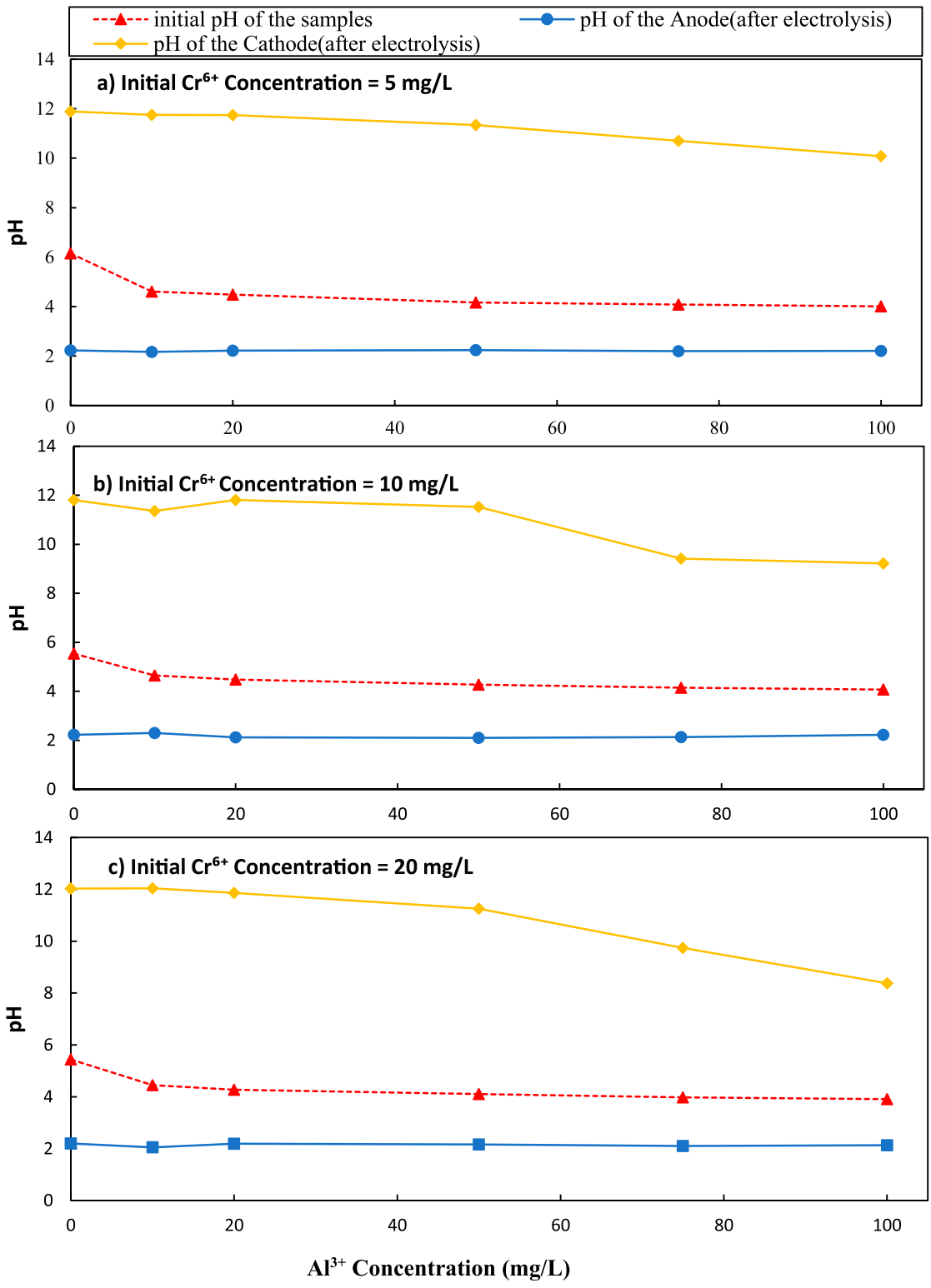

FIGURE 3
Variation of pH with initial Al^{3+} concentration over different initial Cr^{6+} concentration **(a)** 5 mg/L, **(b)** 10 mg/L and **(c)** 20 mg/L C/L applied at = 1500 C/L (0.25A).

According to the results presented in Figures 2a–c, increasing the initial Al^{3+} concentrations increased the precipitate and individual removal efficiencies of Cr^{6+} in both the anode and cathode. In contrast, increased initial Cr^{6+} reduced the removal percentages. Further increasing the initial Al^{3+} concentration also increased removal efficiencies in both the anode and the cathode by

precipitation. The maximum Cr^{6+} removal at the cathode (49.62%), was achieved with an initial Al^{3+} concentration of 100 mg/L at an initial Cr^{6+} concentration of 5 mg/L (Figure 2a) and the respective pH variation can be seen in Figure 3a. This Cr^{6+} removal of 49.62% was a 31.85% increase over the initial level of zero Al^{3+} in the cathode solution ([49.62–31.85] % = coulomb transfer to cathode). However, precipitative removal decreased to 14.24% in the cathode with an initial Al^{3+} concentration of 100 mg/L and an initial Cr^{6+} concentration of 20 mg/L (Figure 2c).

According to Figure 2b, when the Cr^{6+} concentration was 10 mg/L, the maximum Cr^{6+} removal efficiency in the cathode was 19.64%. This level was a 9.76% increase over the initial level of zero Al^{3+} in the solution. When the initial Cr^{6+} concentration was 10 mg/L, the pH was varied from 11.89 to 9.22 for Al^{3+} concentrations of 0–100 mg/L, at the cathode (Figure 3b). According to Figure 2c, when chromium concentration was 20 mg/L, the maximum removal efficiency of Cr^{6+} cathode was 14.64%. This level was a 5.31% increase over the initial zero Al^{3+} level in the solution. When the initial chromium concentration was 20 mg/L, the pH was varied from 11.93 to 8.38 for initial aluminum concentrations of 0–100 mg/L, at the cathode (Figure 3c).

According to Figure 2a, the maximum Cr^{6+} removal by precipitation (68.17%) was achieved for an initial Al^{3+} concentration of 100 mg/L for a 5 mg/L Cr^{6+} concentration. This level was a 69.07% increase over the initial level of Al^{3+} in the solution. When chromium concentration was increased to 10 mg/L, the maximum Cr^{6+} removal by precipitation decreased to 13.68%. Though it was a decreased compared to lower initial Cr^{6+}, 5 mg/L, this level was a 10.50% increase over the initial level of zero Al^{3+} in the solution (Figure 2b). According to Figure 2c, when chromium concentration was 20 mg/L, the maximum Cr^{6+} removal by precipitation was 14.23% which was achieved in the initial Al^{3+} concentration as 100 mg/L. This level was a 12.87% increase over the initial level of zero Al^{3+} in the solution.

The findings indicate that the removal efficiency of Cr^{6+} is strongly dependent on the initial Al^{3+} and Cr^{6+} concentration. At lower Cr^{6+} concentrations, the addition of Al^{3+} significantly improved removal, likely owing to massive production of $Al(OH)_3$ flocs that promote adsorption and sweep coagulation. Yet when the initial concentration of Cr^{6+} is high, the effect becomes less prominent, as a result of the saturation of available binding sites and competitive inhibition by Cr^{6+}. Overall, the results highlight a concentration-dependent synergy between Al^{3+} dosing and electrochemical treatment, with optimal performance observed at lower Cr^{6+} loads and elevated Al^{3+} availability.

Since the overall surface area of $Al(OH)_3$ grows as the initial Al^{3+} concentration rises, the removal of Cr^{6+} should eventually lead to an increase in line with the findings of Figures 2a–c. Here, the concentration of Al^{3+} is increased, and the precipitation of $Al(OH)_3$ occurs in the form of small particles, each of which has a larger surface area to volume ratio. Particulates with a smaller size have greater overall surface area than if the same mass of material is in the form of fewer larger particles. This increase in surface area is important because it determines the number of sites available for binding of Cr^{6+} ions. The adsorption process entails the trapping of Cr^{6+} ions by a cationic surface $Al(OH)_3$, and thus removing them from the solution. Due to the electrolytic effect on the water molecule, the anode effluent's pH reduced as the cathode effluent's pH significantly increased (Figures 3a–c). An oxygen and hydrogen ion are released into the aqueous system as a result of water oxidation caused by the anode, which lowers pH (Equation 2; Equation 3). The interaction of water molecules and electrons in the cathode causes water molecules to dissociate into hydrogen ions and OH^- for high pH (Amarasooriya and Kawakami, 2020; Amarasooriya and Kawakami, 2019).

At the anode

$$H_2O \rightarrow 1/2O_2 + 2H^+ + 2e^- \quad (2)$$

At the cathode

$$2H_2O + 2e^- \rightarrow H_2 + 2OH^- \quad (3)$$

Here, Al^{3+} ions combined with OH^- and generated metallic hydroxides of $Al(OH)_3$, thus hydroxides could remove Cr^{6+} in water. The predominant species of Al^{3+} in the pH range of 5.7–6.7 is $Al(OH)_3$ (Equation 4), and Al^{3+} is predominant at pH less than 5.7.

When the initial chromium concentration was 5 mg/L, the final pH was observed higher than 10, and the value was decreased from 11.80 to 10.08 respectively for initial aluminum concentrations 0–100 mg/L, at the cathode (Figure 3a). At that pH level of, the increment of the pH in cathode lead to generate both $Al(OH)_4^-$ through $Al(OH)_3$ (Equation 4; Equation 5; Equation 6). Accordingly, Cr^{6+} removed by precipitation with both $Al(OH)_3$ and $Al(OH)_4^-$ can be either adsorption or co-precipitation. Electrostatic interactions and surface complexation cause Cr^{6+} ions to be attracted to and retained on the surface of aluminum or its compounds during adsorption. The adsorbed species are further stabilized by the surface reduction of Cr^{6+} to Cr^{3+}. In co-precipitation, it is the simultaneous precipitation of aluminum hydroxide produced during electrolysis and Cr^{3+}, which is reduced from Cr^{6+}. This process is especially important in alkaline environments because aluminum hydroxide is soluble and may co-precipitate to absorb Cr^{3+}.

$$Al^{3+} + 2H_2O \rightarrow Al(OH)_3 + H_2 \quad (4)$$

In bases, it acts as a Lewis acid by binding hydroxide ions,

$$Al(OH)_3 + OH^- \rightarrow Al(OH)_4^- \quad (5)$$

$$Al(OH)_4^- \rightarrow Al(OH)_3 + OH^- \quad (6)$$

One of the most crucial steps in the treatment process is the reduction of hexavalent chromium (Cr^{6+}) into trivalent chromium (Cr^{3+}). In this stage, dichromate ions ($Cr_2O_7^{2-}$) are reduced to Cr^{3+} ions in an acidic reaction medium (Equation 7). This conversion is important because soluble Cr^{6+} is reduced to insoluble Cr^{3+}, which is less soluble and toxic. After forming, Cr^{3+} ions combine with hydroxide ions to generate chromium (III)hydroxide (Equation 8). The reduction of Cr^{6+} to Cr^{3+} was evaluated using a colorimetric method involving ascorbic acid and EDTA, where a significant decrease in the purple-colored complex at 544 nm indicated effective Cr^{6+} reduction. Cr ion is also eliminated from the aqueous phase in the following precipitation of $Cr(OH)_3$, which also yields a solid that can be separated from the solution through filtration. Furthermore, adsorption of dichromate ions on aluminum hydroxide plays an important role in the removal process, as described in Equation 9.

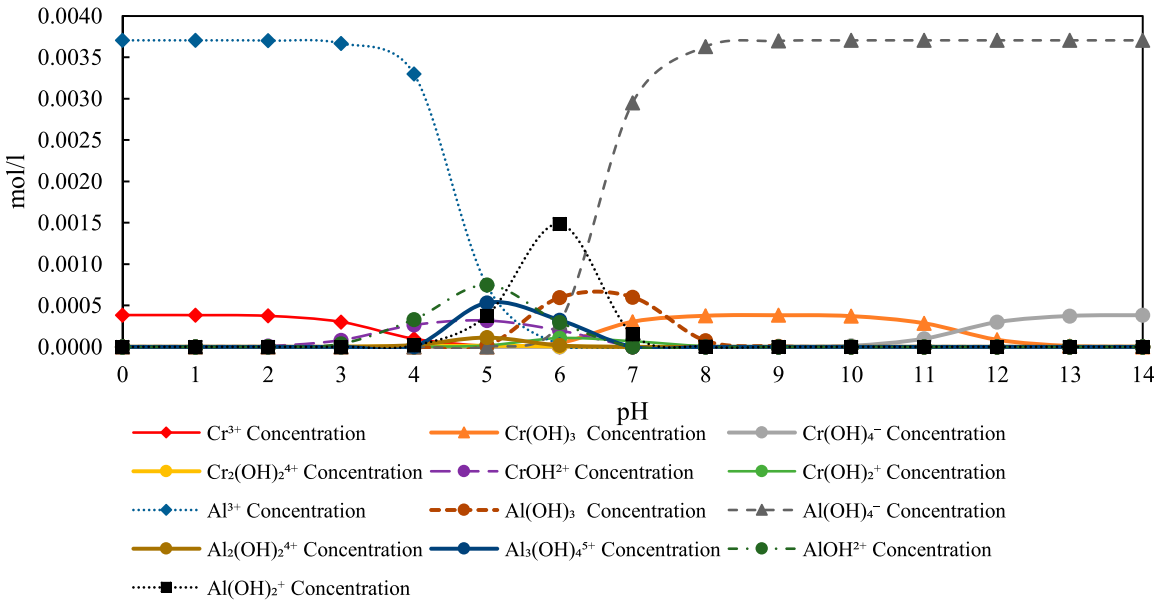

FIGURE 4
Speciation diagram of Al^{3+} Concentration (100 mg/L), Cr^{6+} Concentration (20 mg/L), and related species over pH 0–14 under experimental conditions.

$$Cr_2O_7^{2-}{}_{(aq)} + 14H^+_{(aq)} + 6e^- \rightarrow 2Cr^{3+}_{(aq)} + 7H_2O_{(l)} \quad (7)$$

Co-precipitation of Cr^{3+} with Aluminum Hydroxide:

$$Cr^{3+}_{(aq)} + OH^-_{(aq)} \rightarrow Cr(OH)_{3(S)}\ KSP = 6.3 \times 10^{-31} \quad (8)$$

Adsorption of dichromate Ions on Aluminum hydroxide:

$$\beta Al(OH)_{3(S)} + \alpha Cr_2O_7^{2-}{}_{(aq)} \rightarrow \beta Al(OH)_{3-\alpha/\beta}\, Cr_2O_7^{2-}{}_{(S)} \quad (9)$$

Throughout the experiments involving aluminum ions, the initial pH was not externally adjusted or buffered but allowed to vary naturally, reflecting realistic electrochemical treatment conditions. The cathodic pH increased markedly during electrolysis, ranging from 11.89 at 0 mg/L Al^{3+} to 10.08 at 100 mg/L Al^{3+} (Figure 3a). This pH elevation critically influences the speciation and precipitation behavior of aluminum hydroxides. At near-neutral pH (5.7–6.7), aluminum hydrolyzes to form amorphous $Al(OH)_3$, which possesses a high specific surface area and a positive surface charge, enhancing its ability to adsorb anionic species like chromate (CrO_4^{2-}) and dichromate ($Cr_2O_7^{2-}$). As the pH rises above 9, $Al(OH)_3$ partially dissolves, forming soluble aluminate ions ($Al(OH)_4^-$), which decreases solid-phase adsorption capacity but may facilitate secondary complexation or precipitation mechanisms.

Besides, under acidic to neutral conditions, aluminum released from the anode leads to the formation of amorphous $Al(OH)_3$ flocs, which are positively charged and have a greater surface area. Because of their positive charge, hydroxide ions help capture negatively charged Cr^{6+} oxyanions (such as CrO_4^{2-} and $HCrO_4^-$) by outer-sphere electrostatic attraction. At the same time, when $Al(OH)_3$ and chromate come into contact, ligand exchange between the hydroxyl groups of $Al(OH)_3$ and chromate leads to more specific and stable bonds.

Also, when conditions near the cathode become reducing or intermediates like H_2 gas or electrons appear at the surface, Cr^{6+} adsorbed species usually get reduced to Cr^{3+}, joining the aluminum hydroxide coat or becoming $Cr(OH)_3$. Performing adsorption, reduction, and co-precipitation makes chromium more securely adhered and greatly reduces the release of Cr^{6+} back into the solution.

Higher pH value means that aluminum becomes more likely to be found in the $Al(OH)_4^-$ form. Such complexes may interact with Cr^{3+} ions through ion-pairing or may go back into solid form if close to the cathode, as pH in that area might change. So, keeping the pH in a specific range during electrochemical treatment leads to both a changed appearance and functioning of aluminum hydroxide for taking out chromium.

Because of adsorption and ligand exchange, the reduced Cr^{6+}, with the help of fresh hydroxides, and co-precipitation, the enhanced Cr removal in the electrolysis is easy to explain.

Thermodynamic speciation diagram of aluminum (Al^{3+}), chromium (Cr^{6+}), and their related hydroxide and oxyanion species as a function of pH. Calculations were performed under experimental conditions of 20 mg/L Cr and 100 mg/L Al (Figure 4). The diagram illustrates the dominance of $Al(OH)_3$ and $Al(OH)_4^-$ species in the pH range six to nine, which coincides with the cathodic pH observed in the Al^{3+} system, supporting co-precipitation and adsorption mechanisms for Cr removal.

3.3 Effect of the initial Fe^{3+} concentration on the removal of Cr^{6+}

This section presents the impact of initial Fe^{3+} concentration on the removal efficiency of Cr^{6+} at various Cr^{6+} concentration levels (5 mg/L, 10 mg/L, and 20 mg/L) with a constant charge loading of 1500 C/L

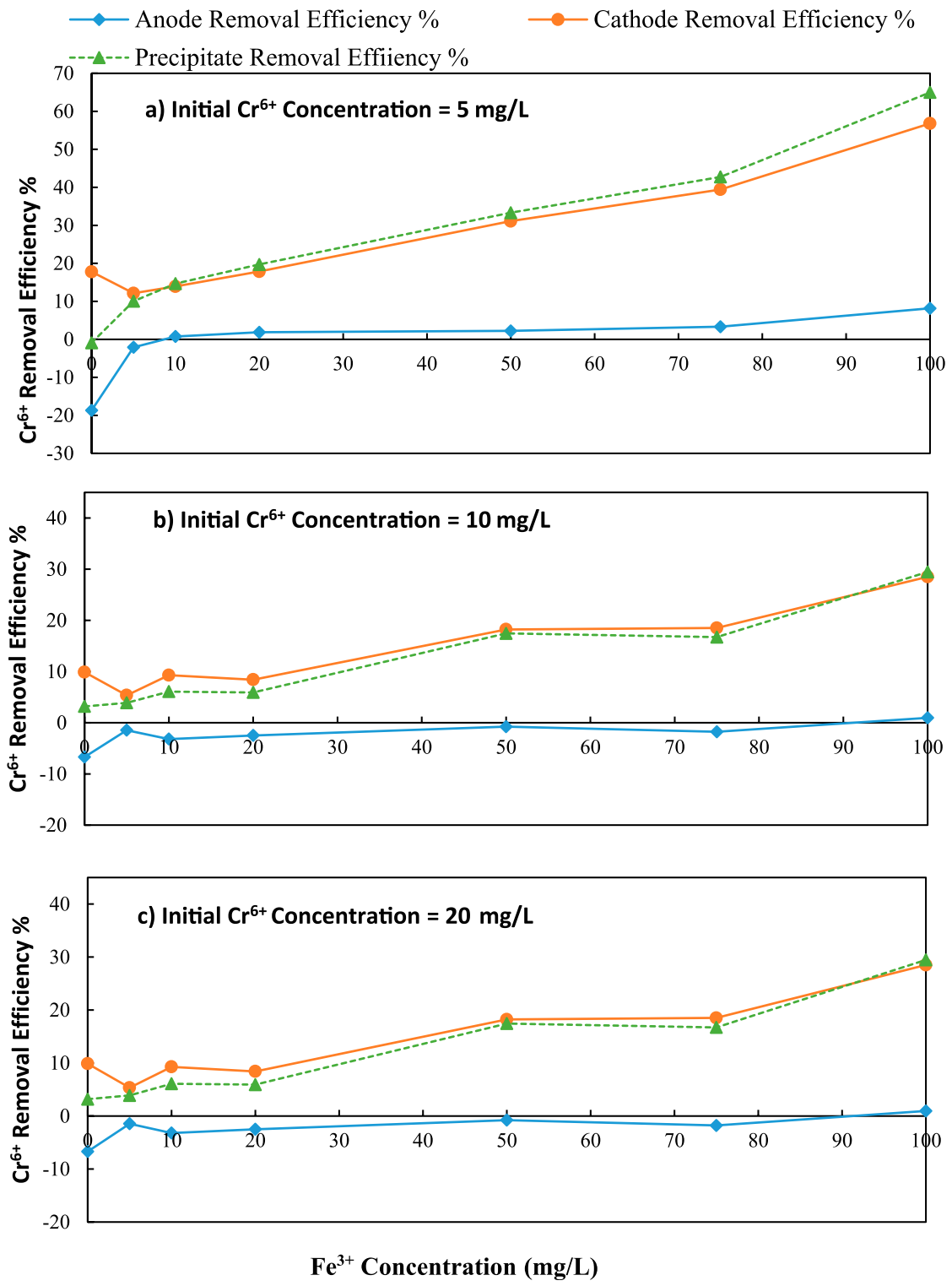

FIGURE 5
Variation of Cr^{6+} removal with initial Fe^{3+} concentration over different initial Cr^{6+} concentration **(a)** 5 mg/L, **(b)** 10 mg/L and **(c)** 20 mg/L; C/L applied at = 1500 C/L (0.25A).

(25 mA for 30 min). Results are shown in Figures 5a–c the initial coagulant (Fe^{3+}) concentrations were varied from 0 mg/L to 100 mg/L for different Cr^{6+} levels. The corresponding pH variations in the anode and cathode baths are shown in Figures 6a–c, respectively.

According to the results presented in Figures 5a–c, an increase in initial Fe^{3+} concentrations increased the precipitation and individual removal efficiencies of Cr^{6+} in both the anode and cathode. However, as the initial Cr^{6+} concentration increased, the total removal

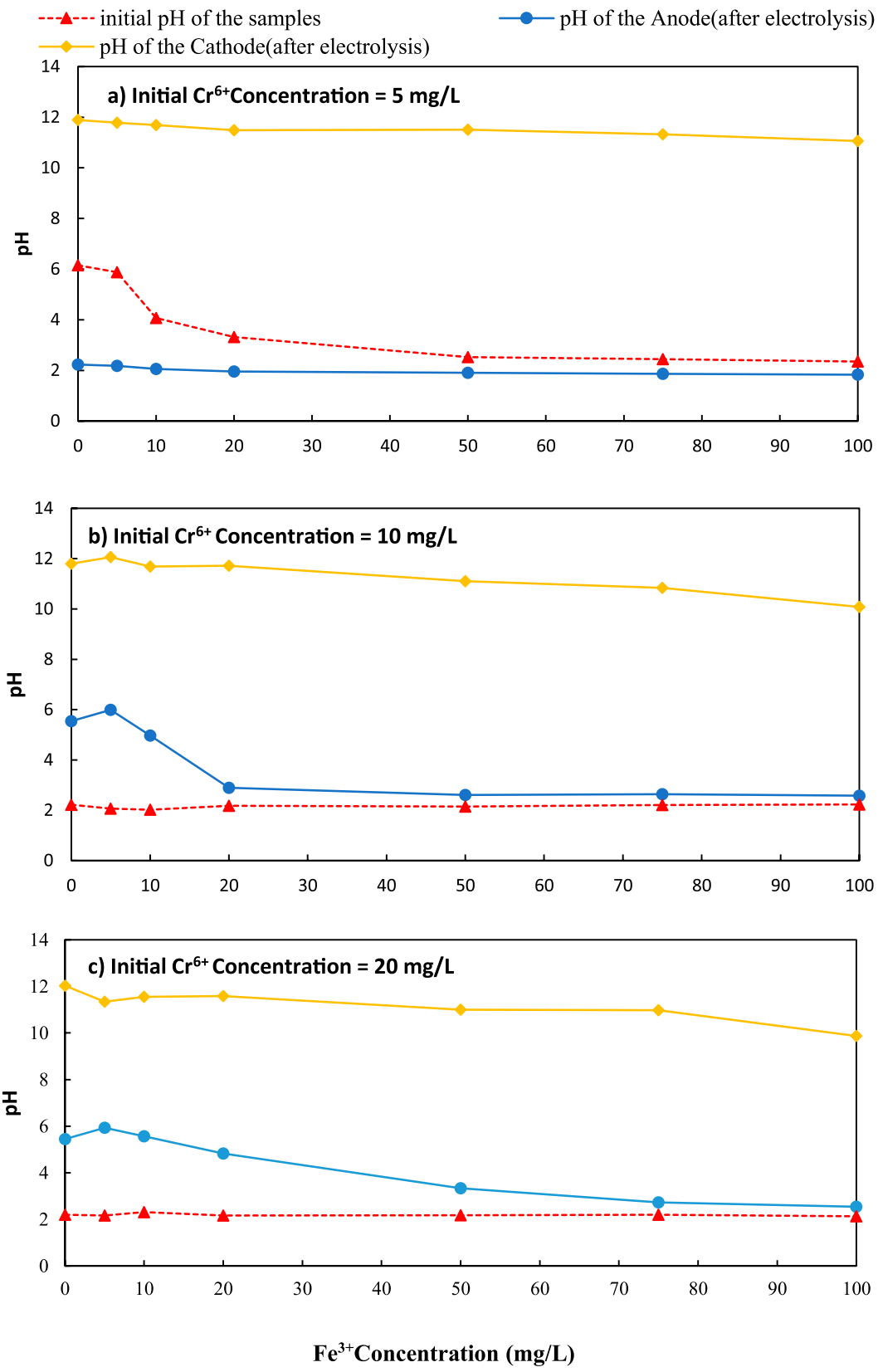

FIGURE 6
Variation of pH with initial Fe^{3+} concentration over different initial Cr^{6+} concentration **(a)** 5 mg/L, **(b)** 10 mg/L and **(c)** 20 mg/L C/L applied at = 1500C/L (0.25A).

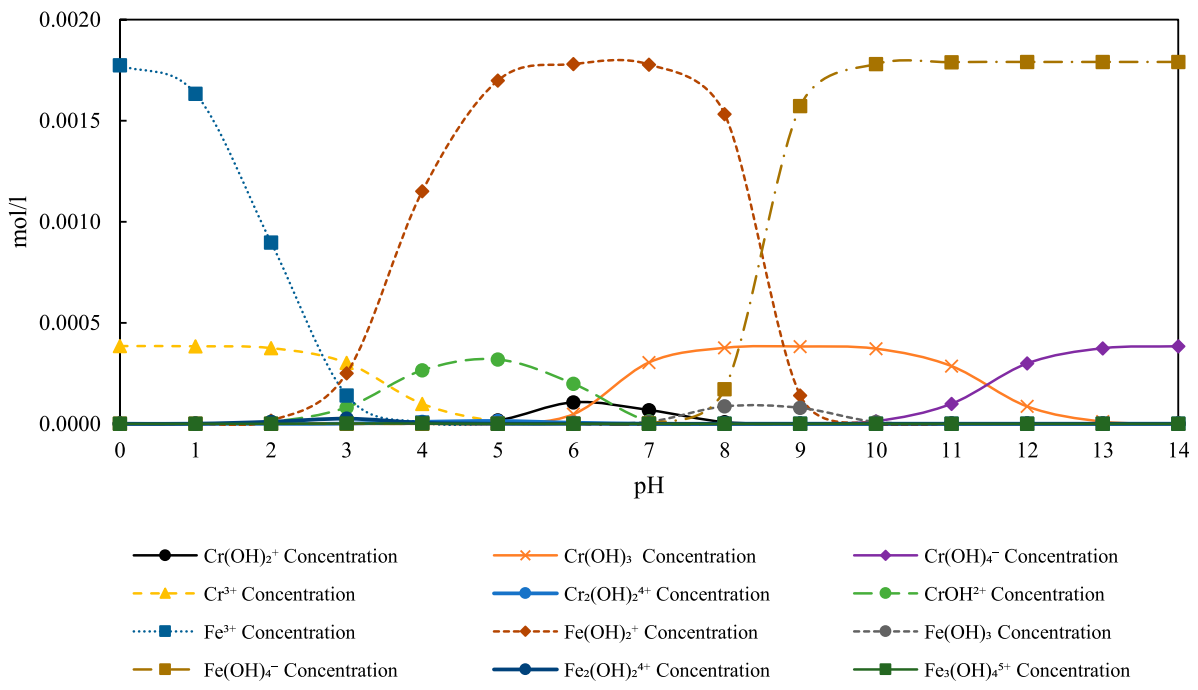

FIGURE 7
Speciation diagram of Fe^{3+} Concentration (100 mg/L), Cr^{6+} Concentration (20 mg/L), and related species over pH 0–14 under experimental conditions.

efficiency of Cr^{6+} decreased. Furthermore, increasing the initial Fe^{3+} concentration also increased the removal efficiency in both the anode and cathode. Equation 1 was employed for calculating the Cr^{6+} removed by precipitation.

The maximum Cr^{6+} removal (56.80%) in the cathode was achieved with an initial Fe^{3+} concentration of 100 mg/L when the initial Cr^{6+} concentration was 5 mg/L. This removal was a 39.03% increase over the initial level of zero Fe^{3+} in the solution (the coulomb transfer caused Cr^{6+} ions to transfer from anode to cathode). When the initial chromium concentration was 5 mg/L, the pH was varied from 11.80 to 11.06 for initial Fe concentrations of 0–100 mg/L, at the cathode (Figure 6a).

According to Figure 5b, when chromium concentration was 10 mg/L, the maximum removal efficiency in the cathode was 28.50% with 100 mg/L of initial Fe^{3+} concentration. This level was an 18.62% increase over the initial level of zero Fe^{3+} in the solution. When the initial chromium concentration was 10 mg/L, the pH was varied from 11.8 to 10.08 for initial Fe concentrations of 0–100 mg/L, at the cathode (Figure 6b).

According to Figure 5c, when chromium concentration was 20 mg/L, the maximum removal efficiency in the cathode was 16.18% with 100 mg/L of initial Fe^{3+} concentration. This level was a 6.87% increase over the initial level of zero Fe^{3+} in the solution. The pH at the cathode was changed from 12.03 to 9.87 for initial Fe concentrations of 0–100 mg/L when the initial concentration of chromium was 20 mg/L (Figure 6c).

The data in Figures 5a,c reveal that the introduction of Fe^{3+} significantly enhanced the removal of Cr^{6+} by precipitation and cathodic reduction. At 5 mg/L Cr^{6+}, the highest overall removal percentage (56.80%) was achieved at 100 mg/L Fe^{3+}, demonstrating efficient sweep flocculation mediated by $Fe(OH)_3$ formation. However, when the initial Cr^{6+} concentration reached 10 mg/L and 20 mg/L, the increase in the removal rate was no longer evident, indicating that the adsorption sites were becoming saturated, and flocs captured decreased. Anodic removal remained consistently low across all conditions, highlighting the dominant role of cathodic and precipitative pathways. These trends reflect a concentration-dependent synergy between Fe^{3+} addition and electrochemical conditions, where optimal Cr^{6+} removal occurs at lower Cr^{6+} loads with sufficient Fe^{3+} to drive co-precipitation and charge neutralization mechanisms.

$Fe(OH)_3$ is the most common form of Fe in the pH range of 8–12 (Stefánsson, 2007).

$$Fe^{3+} + 2H_2O \rightarrow Fe(OH)_3 + H_2 \quad (10)$$

In this instance, Fe^{3+} ions joined with OH^- to form metallic hydroxides of $Fe(OH)_3$, which allowed hydroxides to remove Cr^{6+} from water (Equation 3; Equation 10). $Fe(OH)_3$ is an observed high surface area positive charged material at some pH environments that works well as an adsorbent for negatively charged species such as Cr^{6+} (typically as CrO_4^{2-} or $HCrO_4^-$). The adsorption of Cr^{6+} onto its surface can be enhanced by the presence of $Fe(OH)_3$. Cr^{6+} is frequently converted to Cr^{3+} during electrolysis, particularly when Fe^{2+} or Fe^{3+} ions are present (Equation 7). After that, Cr^{3+} and $Fe(OH)_3$ might co-precipitate to create a mixed hydroxide precipitate. Finally, the adsorption process can help in the additional improvement of hexavalent chromium removal. In the

presence of ferric hydroxide, $Cr_2O_7^{2-}$ ions can be adsorbed onto the ferric hydroxide precipitate (Equation 11).

$$\beta Fe(OH)_{3\,(S)} + \alpha Cr_2O_7^{2-}{}_{(aq)} \rightarrow \beta Fe(OH)_{3-\alpha/\beta}\, Cr_2O_7^{2-}{}_{(S)} \quad (11)$$

Experiments with ferric ions similarly employed unbuffered solutions, permitting cathodic pH to increase naturally from 11.06 to 11.80 across Fe^{3+} concentrations of 0–100 mg/L (Figure 5a). In this alkaline environment, Fe^{3+} rapidly forms $Fe(OH)_3$, a highly porous solid with abundant positively charged surface sites conducive to strong adsorption of CrO_4^{2-} and $Cr_2O_7^{2-}$ through Coulombic forces and ligand exchange.

As $Fe(OH)_3$ is more stable and easily formed at pH values of neutral to slightly alkaline, this procedure is especially successful there. According to the results of Figures 5a–c, the removal of Cr^{6+} should eventually cause an increase as the total surface area of $Fe(OH)_3$ increases as the initial Fe^{3+} concentration rises.

With an initial Fe^{3+} concentration of 100 mg/L, the highest removal of Cr^{6+} by precipitation (64.98%) was achieved in a 5 mg/L Cr^{6+} solution. Over the initial Fe^{3+} concentration in the solution, this amount represented an increase of 65.88% (Figure 6a). When the chromium concentration was 10 mg/L, Figure 6b shows that the maximum removal effectiveness of Cr^{6+} by precipitation was 29.45%. This amount represented a 26.27% increase over the solution's initial Fe^{3+} concentration of zero. According to Figure 6c, when chromium concentration was 20 mg/L, the maximum Cr^{6+} removal by precipitation was 12.24%, achieved in the initial Fe^{3+} concentration of 100 mg/L. This level was a 10.88% increase over the initial level of zero Fe^{3+} in the solution.

While the experimental data demonstrate a clear enhancement in Cr^{6+} removal with increasing Fe^{3+} concentrations, understanding the underlying chemical pathways is essential to explain this behaviour and optimize treatment performance. Cr^{6+} exists in aqueous solutions primarily as the oxyanions chromate (CrO_4^{2-}) and dichromate ($Cr2O_7^{2-}$), which are highly mobile and toxic. When Fe^{3+} ions are introduced into the solution, they rapidly hydrolyse to form $Fe(OH)_3$ precipitates, especially under neutral to slightly alkaline conditions. Because of their large surface area and positive charge in they are suitable for electrostatic reactions.

In addition to adsorption, $Fe(OH)_3$ supports an inner-sphere type of surface complexation between the Cr^{6+} ions and surface OH groups. Where Fe^{2+} forms, either from cathodic reactions or the reduction of Fe^{3+}, a redox reaction occurs that reduces Cr^{6+} to the Cr^{3+} form. Because Cr^{6+} is highly toxic, the transformation to Cr^{3+} and the creation of $Cr(OH)_3$ is necessary, since the new Cr^{3+} is less dangerous and the $Cr(OH)_3$ easily settles out under the conditions. The freshly created $Cr(OH)_3$ may join $Fe(OH)_3$ particles or adsorb onto its surface, which helps take the $CrOH_4$ out of the solution.

Besides, the exchange of Cr^{6+} ions with surface hydroxyls on $Fe(OH)_3$ increases the protection of the sorbed complexes. As a result of this process and mixed-metal hydroxide flocs, the structure of the precipitates becomes better, and the possibility of Cr species moving again is reduced. These mixed precipitates may be made up of Fe–Cr hydroxide networks that give more ways for chromium to be captured.

Because of electrostatic adsorption, redox reduction, and co-precipitation, a higher Fe^{3+} concentration leads to higher removal of Cr^{6+}, which is seen in Figures 6a,c. The process functions best when the solution is somewhat acidic or neutral, since at these levels $Fe(OH)_3$ is both stable and effective. The results validate the experimental findings and show that using active groups of Fe^{3+} plays a key role in optimizing Cr^{6+} removal in electrochemical devices.

Thermodynamic speciation diagram of iron (Fe^{3+}), chromium (Cr^6), and associated hydroxide and oxyanion species versus pH, at 20 mg/L Cr and 100 mg/L Fe^{3+}. The diagram highlights the formation of $Fe(OH)_3$ predominantly between pH six and 9, consistent with measured cathodic pH values, enabling effective Cr removal through precipitation and redox reactions.

3.4 Effect of the initial Mg^{2+} concentration on the removal of Cr^{6+}

Additionally, as shown in Figures 8a–c, this study investigates the effect of initial Mg^{2+} concentration on the removal efficiency of Cr^{6+} at different Cr^{6+} concentrations as 5 mg/L, 10 mg/L, and 20 mg/L with a constant charge loading of 1500 C/L (25 mA for 30 min). The initial Mg^{2+} concentration was varied from 0 mg/L to 100 mg/L. Variation of Cr^{6+} removal in the cathode is shown in Figures 8a–c as a function of initial Mg^{2+} concentration. According to the results, when the initial Mg^{2+} concentrations increased, the removal efficiency of the Cr^{6+} concentration increased.

The maximum Cr^{6+} (Initial Cr^{6+} = 5 mg/L) removal (30.05%) was achieved at the cathode when the initial Mg^{2+} concentration was 100 mg/L. This level was a 12.28% increase over the initial level of zero Mg^{2+} in the solution ([30.05–12.28] % = coulomb transfer to cathode) (Figure 8a). The pH levels of 11.79–11.04 were observed for initial magnesium concentrations of 0–100 mg/L, in an initial chromium concentration was 10 mg/L (Figure 9a).

According to Figure 8b, when the solution chromium concentration was 10 mg/L, the maximum removal efficiency at the cathode was found as 23.78% at 100 mg/L initial Mg^{2+} concentration. This level was a 13.90% increase over the initial level of zero Mg^{2+} in the solution. When the initial chromium concentration was 10 mg/L, the pH was varied from 11.80 to 10.42 for initial magnesium concentrations of 0–100 mg/L, at the cathode (Figure 9b).

According to Figure 8c, when chromium concentration was 20 mg/L, the maximum removal efficiency was 15.87% at 100 mg/L initial Mg^{2+} concentration at the cathode. This level was a 6.56% increase over the initial level of zero Mg^{2+} in the solution. According to the results, the chromium removal efficiency decreased as the initial chromium concentration increased. The pH was varied from 11.93 to 10.86 for initial magnesium concentrations of 0–100 mg/L, and the initial chromium concentration was 20 mg/L at the cathode (Figure 9c).

The Cr^{6+} removal efficiency increased with rising initial Mg^{2+} concentrations at all initial Cr^{6+} levels (5, 10, and 20 mg/L), but the magnitude of improvement diminished as the Cr^{6+} concentration increased. At lower Cr^{6+} concentrations (e.g., 5 mg/L), Mg^{2+} effectively formed $Mg(OH)_2$ flocs that promoted Cr^{6+} removal via adsorption and sweep coagulation,

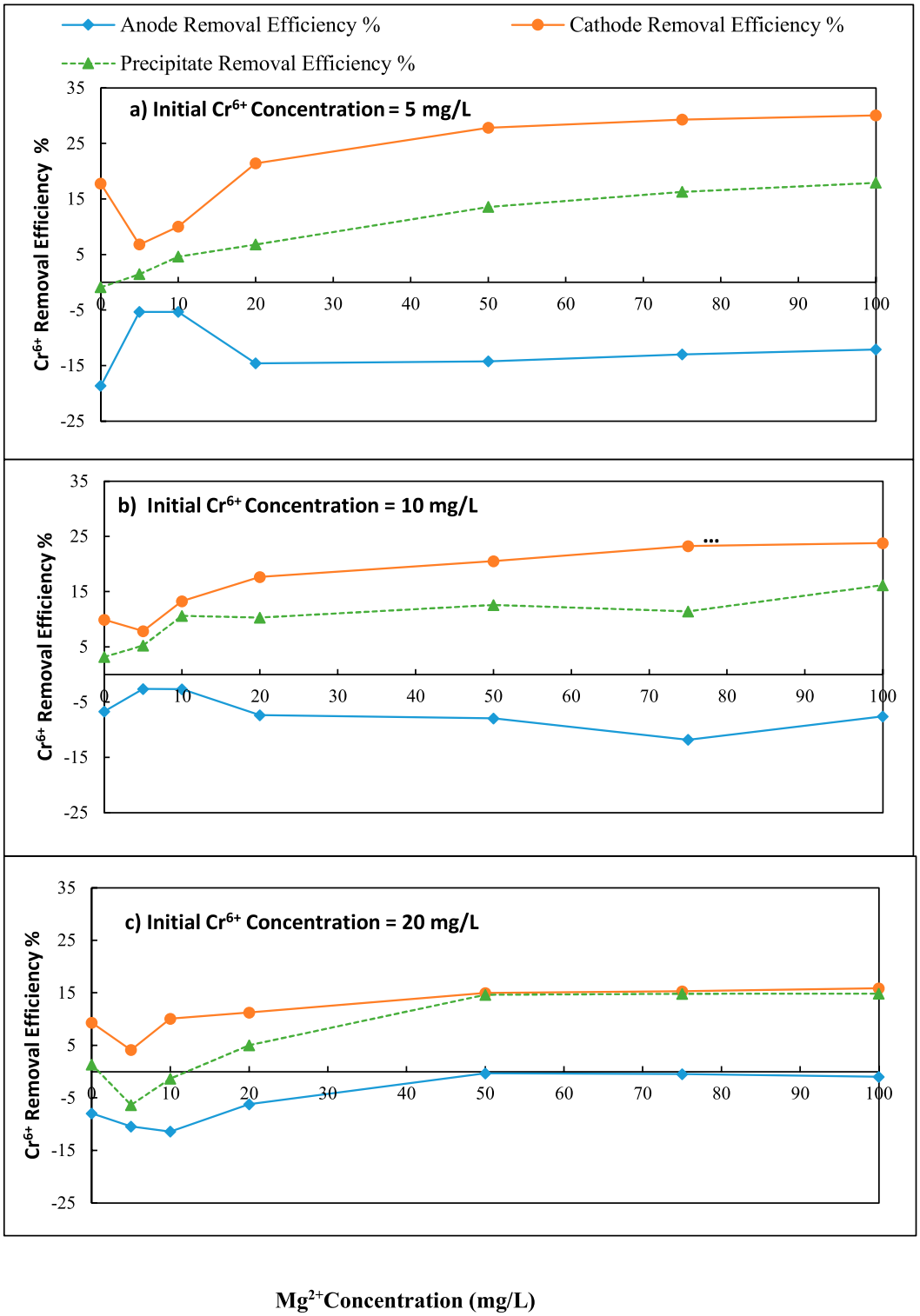

FIGURE 8
Variation of Cr^{6+} removal with initial Mg^{2+} concentration over different initial Cr^{6+} concentration **(a)** 5 mg/L, **(b)** 10 mg/L and **(c)** 20 mg/L; C/L applied at = 1500 C/L (0.25A).

resulting in a maximum removal of 30.05%. However, as initial Cr^{6+} increased to 10 and 20 mg/L, the available $Mg(OH)_2$ became insufficient relative to Cr^{6+} load, leading to floc surface saturation and reduced removal efficiency. Additionally, the gradual decrease in pH observed with increasing Mg^{2+} may have reduced the formation and stability of hydroxide flocs, further impacting performance. These findings highlight a concentration-dependent trend, where Mg^{2+} dosing is most

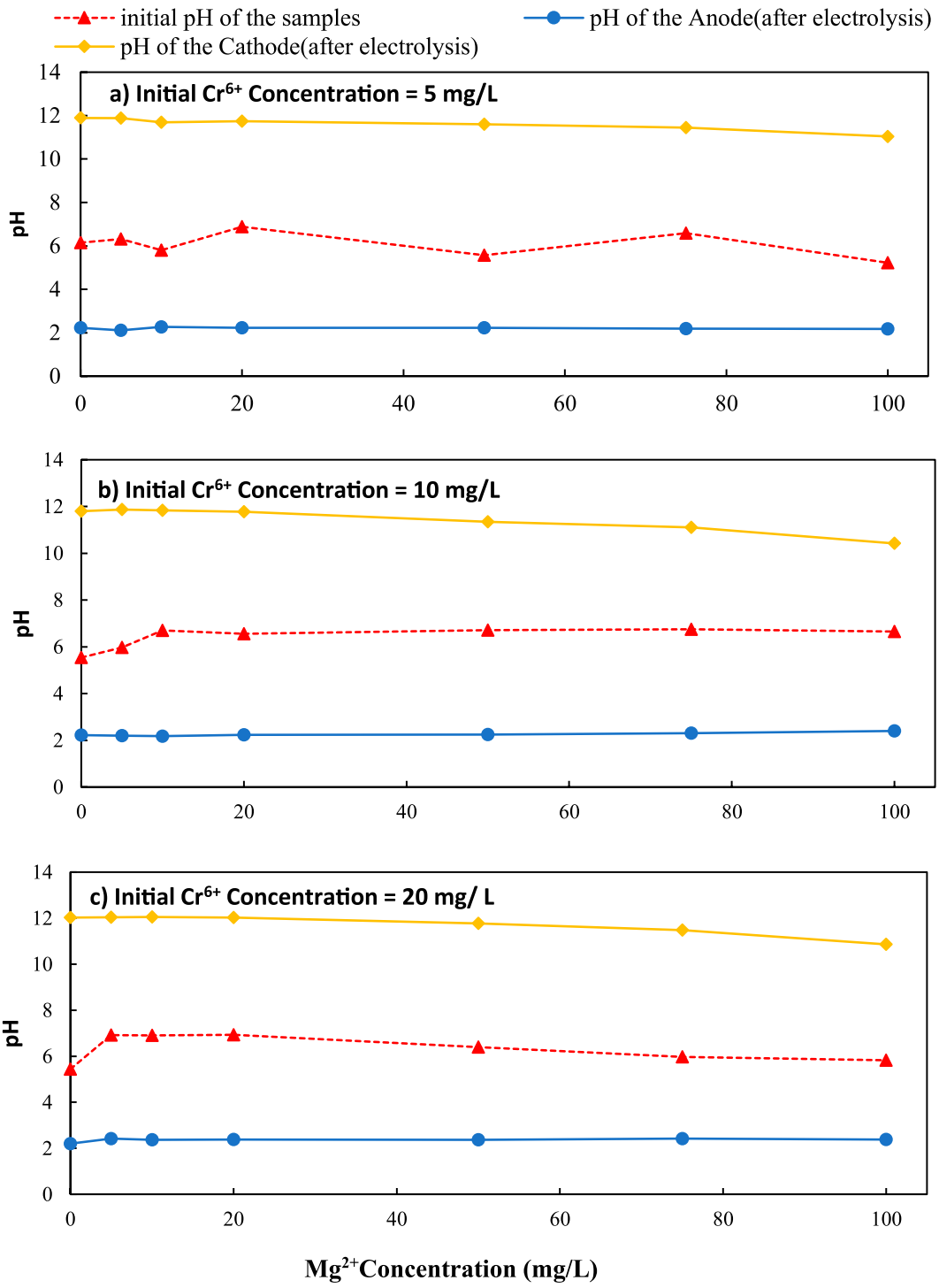

FIGURE 9
Variation of pH with initial Mg^{2+} concentration over different initial Cr^{6+} concentration **(a)** 5 mg/L, **(b)** 10 mg/L and **(c)** 20 mg/L C/L applied at = 1500 C/L (0.25A)

effective at lower Cr^{6+} concentrations and is limited by charge imbalance and floc capacity at higher contaminant loads.

The predominant species of Mg^{2+} in the pH range of 8.7–12.5 is $Mg(OH)_2$.

$$Mg^{2+} + 2H_2O \rightarrow Mg(OH)_2 + H_2 \quad (12)$$

Magnesium experiments were conducted under similar unbuffered conditions, with cathodic pH rising from 10.86 to 12.03 as Mg^{2+} concentrations increased from 0 to 100 mg/L (Figure 9c). Above pH 9, Mg^{2+} precipitates as $Mg(OH)_2$, a crystalline phase characterized by lower surface charge and

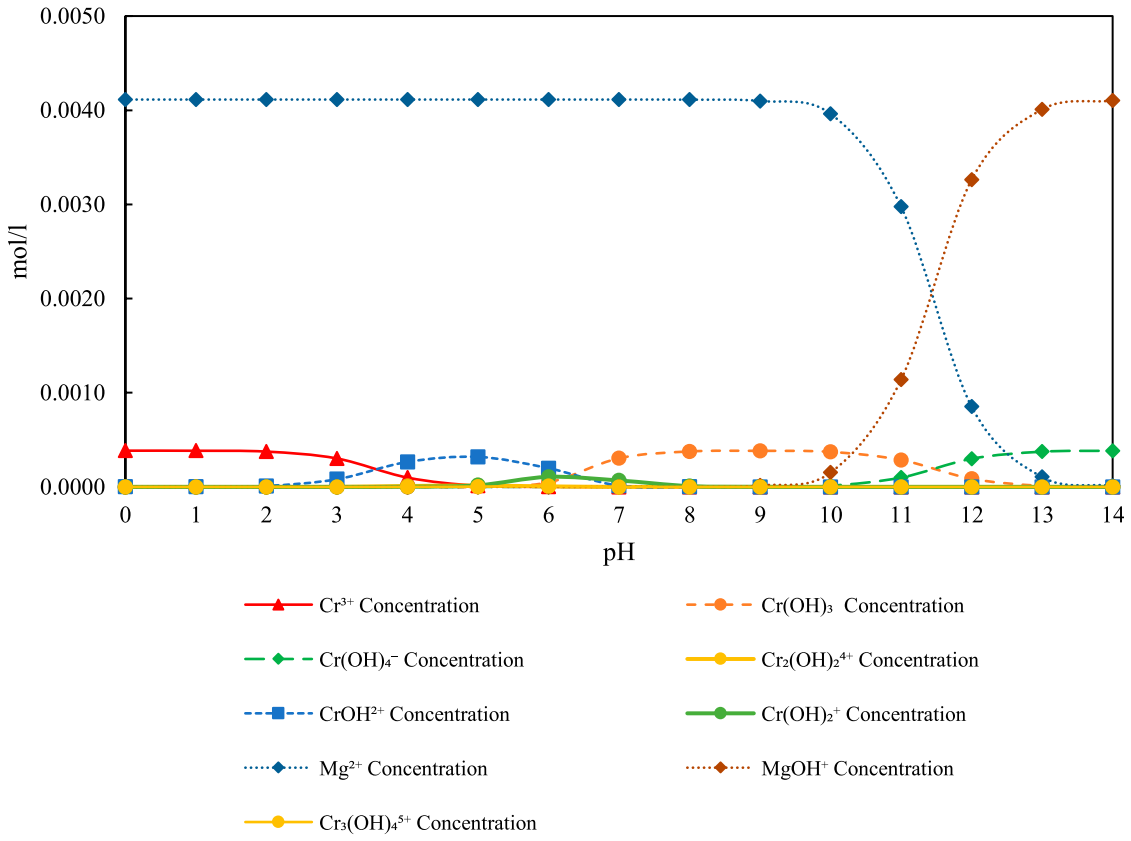

FIGURE 10
Speciation diagram of Mg^{2+} Concentration (100 mg/L), Cr^{6+} Concentration (20 mg/L), and related species over pH 0–14 under experimental conditions.

adsorption capacity compared to amorphous $Al(OH)_3$ and $Fe(OH)_3$.

Here, Mg^{2+} ions interacted with OH^- to generate $Mg(OH)_3$ metallic hydroxides, which allowed hydroxides to remove Cr^{6+} from water (Equation 3; Equation 12).

The pH change for different initial Mg^{2+} concentrations is shown in Figures 9a–c. The pH levels of 11.79–11.04 were observed for initial magnesium concentrations of 0–100 mg/L; hence predominant species is $Mg(OH)_2$. The formation of $Mg(OH)_2$ could lead to Cr co-precipitation or adsorption on the surface (Equation 8; Equation 13).

Adsorption of Dichromate Ions on Magnesium Hydroxide:

$$\beta Mg(OH)_{2(S)} + \alpha Cr_2O_7^{2-}{}_{(aq)} \rightarrow \beta Mg(OH)_{2-\alpha/\beta}\, Cr_2O_7^{2-}{}_{(S)} \quad (13)$$

The overall surface area of $Mg(OH)_2$ grows as the initial Mg^{2+} concentration rises. Thus, the removal of Cr^{6+} should eventually lead to an increase in line with the findings of Figures 8a–c, $Mg(OH)_2$ generation increased with increasing initial Mg^{2+} concentration, increasing Cr^{6+} removal as a form of precipitate in the cathode, and increasing the gradient of Cr^{6+} ion concentration between the cathode and anode. Hence, the Cr^{6+} removal by co-precipitation was increased. The maximum Cr^{6+} removal by precipitation (17.91%) was achieved with an initial Mg concentration of 100 mg/L (Figure 8a). This level was an 18.81% increase over the initial level of zero Mg^{2+} in the solution. According to Figure 8b, when chromium concentration was 10 mg/L, the maximum Cr^{6+} removal by precipitation removal efficiency was 16.18%. This level was a 13.00% increase over the initial level of zero Mg^{2+} in the solution. According to Figure 8c, when chromium concentration was 20 mg/L, the maximum Cr^{6+} removal by precipitation was 14.86%, achieved in an initial Mg^{2+} concentration of 100 mg/L. This level was a 13.50% increase over the initial level of zero Mg^{2+} in the solution.

At a mechanistic level, the interaction between Cr^{6+} species and $Mg(OH)_2$ involves a combination of surface chemistry, solid-phase equilibria, and ionic strength effects under alkaline conditions. $Mg(OH)_2$, crystallizing in a brucite-type structure, has surface hydroxyl moieties (≡Mg–OH) that are subject to protonation–deprotonation under the influence of the pH of the solution, imparting surface charge. At a pH level above 10, the surface exhibits either a neutral or slightly positive charge, which enables a selective adsorption of Cr^{6+} anions through inner-sphere complexation, wherein the dichromate or chromate species displace surface hydroxyls via ligand exchange. The interaction is thermodynamically favoured in high-pH, low-buffering environments in that the dissolution of $Mg(OH)_2$ is kept very low to the extent of occurrence of a stable solid phase. The interaction can also take place through partial incorporation of chromium into the lattice of $Mg(OH)_2$, and at least in the early stages of precipitation, under very fast nucleation, hydroxide

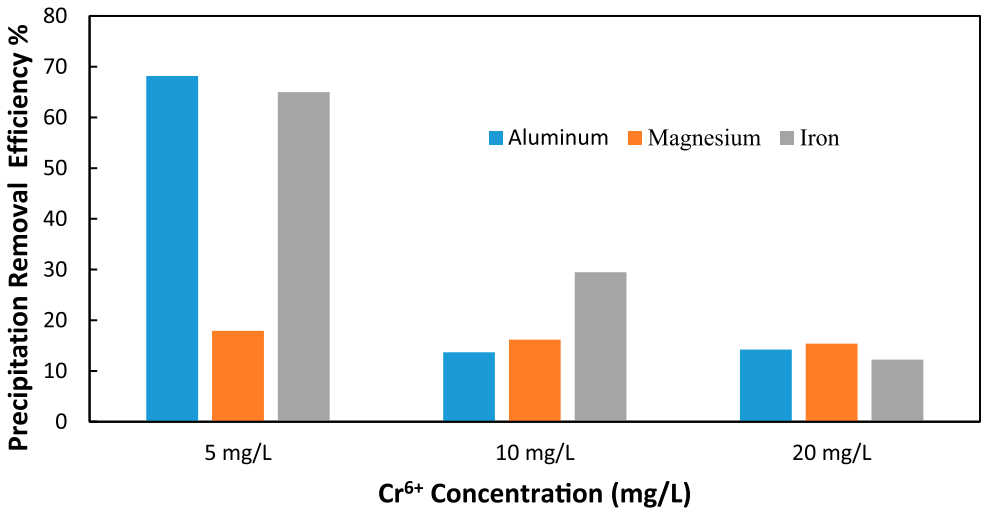

FIGURE 11
Comparison of Al^{3+} (100 mg/L), Mg^{2+} (100 mg/L), and Fe^{3+} (100 mg/L) Ion Additives on Cr^{6+} Precipitation Removal Efficiency at Different Cr^{6+} Levels (5 mg/L, 10 mg/L, and 20 mg/L) and c) 20 mg/L (C/L applied at = 1500 C/L (0.25 A).

precipitation is capable of entrapping Cr^{6+} ions. Although $Mg(OH)_2$ has a lower charge density on the surface relative to $Fe(OH)_3$ or $Al(OH)_3$, the structural stability of $Mg(OH)_2$ increases, together with its surface area as the concentrations of Mg^{2+} increase, thereby providing potential removal power continually and cumulatively. The enhancement of the overall driving force for both adsorption and entrapment could also be attributed to the creation of local microenvironments around the cathode that subsequently give rise to a diffusion gradient favouring Cr^{6+} migration and immobilization.

Thermodynamic speciation diagram of magnesium (Mg^{2+}), chromium (Cr^{6+}), and their related hydroxide and complex species as a function of pH, modeled for 20 mg/L Cr and 100 mg/L Mg (Figure 10). The figure shows that $Mg(OH)_2$ becomes dominant above pH 10, in agreement with cathodic pH measurements, facilitating Cr removal via surface complexation and entrapment mechanisms.

3.5 Comparison of maximum removal efficiencies

From the study, according to Figure 11, it is demonstrated that at the lowest Cr^{6+} concentration of 5 mg/L, Al^{3+} (100 mg/L) is highly preferred in the precipitation of Cr^{6+} with nearly 70% precipitation efficiency. This high performance indicates that Al^{3+} ions may also contribute greatly to the enhancement of Cr^{6+} removal via the formation of soluble complexes or co-precipitate. Similarly, to Fe^{3+} (100 mg/L), the removal efficiency increases to a maximum of over 65% at this concentration, proving that it could be an effective candidate for chromium precipitation. However, Mg^{2+} (100 mg/L) has a significantly poor performance as its removal efficiency is nearly 15%, which could mean that its contribution towards the Cr^{6+} precipitation is not as efficient as other ions at this concentration.

When the concentration of Cr^{6+} reaches 10 mg/L, it can be observed that the removal percentage of each ion additive decreases. Thus, Fe^{3+} remains the most efficient ion, even though its efficiency is only 35% compared to the maximum values. This indicates that although Fe^{3+} is still involved in the removal of Cr^{6+}, its effectiveness depends on its concentration. At this concentration, both Al^{3+} and Mg^{2+} have nearly the same efficiency, which varies between 10%–15%. This decrease, especially in Al^{3+}, means that, as the concentration increases, the ion's ability to promote Cr^{6+} precipitation decreases, possibly because of saturation and other impacts on competitive precipitation mechanisms that may occur after adding more Cr^{6+} into the solution.

When the Cr^{6+} ion concentration increases to the highest level of 20 mg/L, the removal efficiencies of all ions are reduced. As for the efficiency of Al^{3+}, $Mg^{2+,}$ and Fe^{3+}, the values defined and calculated reach almost the same numbers, equal to 10% and less than 10%, respectively, for every ion. At these higher concentrations, therefore, the present results indicate that the ability of each ion to precipitate Cr^{6+} may be constrained. The marked decrease in efficiency, especially in Al^{3+} and Fe^{3+}, suggests that increased Cr^{6+} concentrations present certain difficulties to the precipitation process, either due to the lower availability of reactive sites or due to the enhanced complexity of interactions in solution.

Among the cations, Al^{3+} and Fe^{3+} are found to be the most effective ions to be used as additives for chromium ions at low initial concentrations of 5 mg/L of Cr^{6+} and varying pH levels, with Al^{3+} being the most efficient. Al^{3+} and Fe^{3+} removal rate decreases significantly with the increase in the concentration of Cr^{6+} in the solution, and reveals a strong concentration dependency of Cr^{6+}. At the same time, the data clearly illustrate that Mg^{2+} has the lowest removal efficiency in all the concentrations and, therefore, appears to be the least efficient in promoting Cr^{6+} precipitation under the tested conditions.

The relevance of these outcomes is emphasized by the importance of enhancing the electrolysis-based Cr^{6+} removal processes. With the high performance of Al^{3+} at lower concentrations, it could be used as an additive where the trace of Cr^{6+} is present or in areas where Cr^{6+} concentrations are still

relatively low. Currently, for high chromium concentration, it may be useful to develop new techniques or apply more than one additive to facilitate the improvement of Cr^{6+} removal efficiency.

Compared to existing studies on this study provides a unique assessment of Cr^{6+} removal by systematically evaluating and comparing the electrocoagulation removal efficiencies of potential coagulant additive ions (Al^{3+}, Fe^{3+}, and Mg^{2+}) under the same conditions, rather than conducting simple operational comparisons and other constraints discussed earlier. Prior studies were able to attain high Cr^{6+} removal efficiencies through electrocoagulation or chemical precipitation processes individually, but none were easily found as explicit side-by-side comparisons of different coagulant ions in a single electrolysis treatment study. In this study, Al^{3+}-mediated precipitation offers some of the highest Cr^{6+} removal, which also includes cathodic precipitation at 68.17% and 49.62%, respectively, with comparable treatment times (30 min) and charge loadings (1500 C/L) for other experimental ions. The reported Cr^{6+} removal efficiencies were not from the samples using either coagulant, nor adjusting sample volumes, and therefore the voltages and overall treatment times were higher, which are presumably inefficient and potentially not commercially scalable. Additionally, the concentration-dependent removal efficiencies and mechanisms described here, along with the influence of pH, coagulant dose, and Cr^{6+} loading, elaborated more detailed and diverse studies to provide a thorough review of the conditions influencing the conductivity of Cr^{6+} with various coagulant ions, which other works do not typically consider. It is expected that such coupling of an electrochemical process can be designed in such a way as to produce even better results. Therefore, this study has many distinct advantages and is a notably comprehensive and practically useful reference to optimize Cr^{6+} removal issues related to electrochemical-coagulant coupling.

3.6 Practical implications and scalability for industrial application

The batch electrolysis system demonstrated effective Cr^{6+} removal at the laboratory scale, indicating promising potential for industrial wastewater treatment applications. However, applying these techniques in real-world applications requires careful consideration of several technical and economic factors. Energy consumption is a key determinant of feasibility; although the current applied here (0.25 A) is modest, scaling to higher volumes will proportionally increase power requirements. The energy consumption for Cr^{6+} removal was estimated to be between 1.4 and 3.5 kWh per cubic meter of treated water, corresponding to an operational cost of approximately USD 0.25 to USD 0.63 (LKR 75–189) per cubic meter. These findings demonstrate the process's potential for energy-efficient electrochemical remediation. Optimizing current density and cell design can improve energy efficiency, but requires pilot-scale studies. The selection of electrode materials and their longevity have a significant impact on operational costs and maintenance frequency. The use of a platinum anode, while effective and inert, is expensive, potentially limiting commercial viability; thus, exploring alternative, cost-effective anode materials with similar stability is recommended. Stainless steel cathodes offer durability but may experience corrosion or fouling issues over extended use, which can affect removal efficiency. The generation and management of metal hydroxide sludge ($Al(OH)_3$, $Fe(OH)_3$, $Mg(OH)_2$) pose environmental and operational challenges. Proper handling, dewatering, and safe disposal or recovery of chromium-laden sludge must be integrated into the treatment workflow to avoid secondary pollution. Wastewater variability, including fluctuating Cr^{6+} concentrations, pH, and presence of competing ions, can influence system performance; thus, adaptive operational controls will be necessary. Integration with existing treatment processes, such as sedimentation tanks or filtration units, could enhance overall system efficacy and feasibility. To advance from laboratory to industrial scale, future research should focus on continuous-flow reactor designs, long-term electrode stability testing, energy consumption optimization, and comprehensive cost-benefit analyses. Such efforts will clarify the method's practical potential and guide engineering development for large-scale chromium remediation.

4 Conclusion

This study investigated the electrolysis system to optimize the removal of Cr^{6+} from wastewater using a platinum anode and a stainless-steel cathode. The effectiveness of the electrolysis system in removing Cr^{6+} at various concentrations (5mg/L-100 mg/L) of Al^{3+}, Fe^{3+}, and Mg^{2+} was examined. Results indicated that even in the absence of Al^{3+}, Fe^{3+}, and Mg^{2+}, the system could remove Cr^{6+} through Coulomb forces and precipitation. However, the presence of these additives markedly enhanced removal efficiency through co-precipitation with their respective hydroxides ($Al(OH)_3$, $Fe(OH)_3$, and $Mg(OH)_2$). The observed decline in removal efficiency at higher initial Cr^{6+} concentrations is attributed to the saturation of hydroxide binding sites and limited charge transfer capacity inherent to the system.

With an initial Al^{3+} concentration of 100 mg/L and an initial Cr^{6+} concentration of 5 mg/L, the maximum Cr^{6+} removal achieved was 49.62%, representing a 31.85% increase compared to the solution with zero initial Al^{3+} concentration. Similarly, with an initial Fe^{3+} concentration of 100 mg/L and an initial Cr^{6+} concentration of 5 mg/L, the maximum Cr^{6+} removal observed was 56.80%, a 39.03% increase over the solution with zero initial Fe^{3+} concentration. The highest removal of Cr^{6+} (30.05%) was achieved with an initial Mg^{2+} concentration of 100 mg/L and an initial Cr^{6+} concentration of 5 mg/L, showing a 12.28% increase compared to the solution with zero initial Mg^{2+} concentration.

Building upon these findings, future research should explore a wider spectrum of multivalent additives such as Ca^{2+}, Zn^{2+}, Mn^{2+}, and Cu^{2+}, which may form hydroxides with distinct surface properties conducive to improved adsorption and coagulation. Studies on synergistic effects of the binary or ternary combinations of additives will also highlight removal efficiencies that surpass those obtained using single additives. In another direction, optimization of operational parameters such as current density, pH, and electrolyte composition, through modern statistical tools like response surface methodology, may provide other possible improvements.

Given the similarities in removal mechanisms, most notably involving adsorption, precipitation, and redox transformations, the presented electrochemical platform would also be promising for the removal of the heavy metals lead (Pb^{2+}), cadmium (Cd^{2+}), nickel (Ni^{2+}), and arsenic (As^{5+}). More importantly, validation of this system for the treatment of real industrial wastewater, which has complex matrices and competing ions among others, will be critical in assessing its robustness and hence, applicability in a practical scenario.

For system scalability and field deployment, stepping up from batch experiments to flows or pilots is crucial when it comes to testing energy recovery efficiency, electrode stability, sludge disposal and long-term operational feasibility. Another promising prospect for sustainable decentralized wastewater treatment is supposed to be the integration with renewable power generation, i.e., solar or wind. This study confirmed the removal feasibility of Cr^{6+} by additive-enhanced electrolysis and laid down an exhaustive basis for future studies towards improving treatment efficiency, broadening the scope to other contaminants, and advancing scalable and environmentally sustainable wastewater remediation technologies.

Data availability statement

The original contributions presented in the study are included in the article/supplementary material, further inquiries can be directed to the corresponding author.

Author contributions

ST: Data curation, Investigation, Methodology, Visualization, Writing – original draft, Writing – review and editing, Formal Analysis. AG: Conceptualization, Formal Analysis, Methodology, Supervision, Validation, Writing – original draft, Writing – review and editing. TK: Supervision, Writing – review and editing. VS: Writing – original draft, Writing – review and editing, Formal Analysis. GS: Supervision, Writing – original draft, Writing – review and editing.

Funding

The author(s) declare that no financial support was received for the research and/or publication of this article.

Conflict of interest

Author VS was employed by Sweco Norge AS.

The remaining authors declare that the research was conducted in the absence of any commercial or financial relationships that could be construed as a potential conflict of interest.

Generative AI statement

The author(s) declare that no Generative AI was used in the creation of this manuscript.

Publisher's note

References

Aitio, A., Järvisalo, J., Kiilunen, M., Tossavainen, A., and Vaittinen, P. (1984). Urinary excretion of chromium as an indicator of exposure to trivalent chromium sulphate in leather tanning. *Int. Archives Occup. Environ. Health* 54 (3), 241–249. doi:10.1007/BF00379053

Amarasooriya, A. A. G. D., and Kawakami, T. (2019). Removal of fluoride, hardness and alkalinity from groundwater by electrolysis. *Groundw. Sustain. Dev.* 9, 100231. doi:10.1016/j.gsd.2019.100231

Amarasooriya, A. A. G. D., and Kawakami, T. (2020). Removal of co-existing fluoride, calcium, magnesium, and carbonates, by non-chemical induced electrolysis system for drinking and industrial purposes. *H2Open J.* 3 (1), 10–31. doi:10.2166/h2oj.2020.022

Carneiro, J., Tobaldi, D. M., Capela, M. N., Seabra, M. P., and Labrincha, J. A. (2019). Waste-based pigments for application in ceramic glazes and stoneware bodies. *Materials* 12 (20), 3396. doi:10.3390/ma12203396

Characterization, S., Genawi, N. M., Ibrahim, M. H., and El-naas, M. H. (2020). Chromium removal from tannery wastewater by electrocoagulation: optimization and.

Chen, Z., Chen, Y., Liang, J., Sun, Z., Zhao, H., and Huang, Y. (2024). The release and migration of Cr in the soil under alternating wet–dry conditions. *Toxics* 12 (2), 140. doi:10.3390/toxics12020140

Costa, M. (2003). Potential hazards of hexavalent chromate in our drinking water. *Toxicol. Appl. Pharmacol.* 188 (1), 1–5. doi:10.1016/S0041-008X(03)00011-5

Garg, R., Garg, R., Sillanpää, M. A., Khan, M. A., Mubarak, N. M., Tan, Y. H., et al. (2023). Rapid adsorptive removal of chromium from wastewater using walnut-derived biosorbents. *Sci. Rep.* 13 (1), 6859–12. doi:10.1038/s41598-023-33843-3

Golder, A. K., Samanta, A. N., and Ray, S. (2007). Removal of trivalent chromium by electrocoagulation. *Sep. Purif. Technol.* 53 (1), 33–41. doi:10.1016/j.seppur.2006.06.010

Hamadeen, H. M., Elkhatib, E. A., and Moharem, M. L. (2022). Optimization and mechanisms of rapid adsorptive removal of chromium (VI) from wastewater using industrial waste derived nanoparticles. *Sci. Rep.* 12 (1), 14174–12. doi:10.1038/s41598-022-18494-0

Kerur, S. S., Bandekar, S., Hanagadakar, M. S., Nandi, S. S., Ratnamala, G. M., and Hegde, P. G. (2020). Removal of hexavalent Chromium-Industry treated water and Wastewater: a review. *Mater. Today Proc.* 42, 1112–1121. doi:10.1016/j.matpr.2020.12.492

Kokkinos, E., Proskynitopoulou, V., and Zouboulis, A. (2019). Chromium and energy recovery from tannery wastewater treatment waste: Investigation of major mechanisms in the framework of circular economy. *J. Environ. Chem. Eng.* 7 (5), 103307. doi:10.1016/j.jece.2019.103307

Krishnani, K. K., Srinives, S., Mohapatra, B. C., Boddu, V. M., Hao, J., Meng, X., et al. (2013). Hexavalent chromium removal mechanism using conducting polymers. *J. Hazard. Mater.* 252–253, 99–106. doi:10.1016/j.jhazmat.2013.01.079

Kumar Saha, S., and Ghosh, D. (2022). A comprehensive review on toxicity of chromium in freshwater fishes. *Appl. Ecol. Environ. Sci.* 10 (8), 527–533. doi:10.12691/aees-10-8-5

Malinovic, B., Djuricic, T., and Bjelic, D. (2022). Electrochemical removal of hexavalent chromium by. *January*. doi:10.5281/zenodo.6918321

Merical, J. (2007). *The effects and processes for removal of chromium in activated sludge treatment*, 1–11.

Mohan, D., and Pittman, C. U. (2006). Activated carbons and low cost adsorbents for remediation of tri- and hexavalent chromium from water. *J. Hazard. Mater.* 137 (2), 762–811. doi:10.1016/j.jhazmat.2006.06.060

Park, J. E., Shin, J. H., Oh, W., Choi, S. J., Kim, J., Kim, C., et al. (2022). Removal of hexavalent chromium(VI) from wastewater using chitosan-coated iron oxide nanocomposite membranes. *Toxics* 10 (2), 98. doi:10.3390/toxics10020098

Peng, H., Leng, Y., and Guo, J. (2019). Electrochemical removal of chromium (VI) from wastewater. *Appl. Sci. Switz.* 9 (6), 1156. doi:10.3390/app9061156

Stefánsson, A. (2007). Iron (III) hydrolysis and solubility at 25 degrees C. *Environ. Sci. and Technol.* 41 (17), 6117–6123. doi:10.1021/es070174h

Yan, G., Gao, Y., Xue, K., Qi, Y., Fan, Y., Tian, X., et al. (2023). Toxicity mechanisms and remediation strategies for chromium exposure in the environment. *Front. Environ. Sci.* 11 (February), 1–10. doi:10.3389/fenvs.2023.1131204

Yogeshwaran, V., and Priya, A. K. (2018). Removal of hexavalent chromium (Cr6) using different natural adsorbents A review. *SSRN Electron. J.*, 1–20. doi:10.2139/ssrn.3090245

Zhou, J., Du, N., Li, D., Qin, J., Li, H., and Chen, G. (2021). Combined effects of perchlorate and hexavalent chromium on the survival, growth and reproduction of Daphnia carinata. *Sci. Total Environ.* 769, 144676. doi:10.1016/j.scitotenv.2020.144676

Zongo, I., Leclerc, J., Amadou, H., Wéthé, J., and Lapicque, F. (2009). Removal of hexavalent chromium from industrial wastewater by electrocoagulation: a comprehensive comparison of aluminium and iron electrodes. 66, 159–166. doi:10.1016/j.seppur.2008.11.012